

Centrality Dependence of the Charged-Particle Multiplicity Density at Midrapidity in Pb-Pb Collisions at $\sqrt{s_{\text{NN}}} = 2.76$ TeV

K. Aamodt *et al.**

(ALICE Collaboration)

(Received 8 December 2010; published 20 January 2011)

The centrality dependence of the charged-particle multiplicity density at midrapidity in Pb-Pb collisions at $\sqrt{s_{\text{NN}}} = 2.76$ TeV is presented. The charged-particle density normalized per participating nucleon pair increases by about a factor of 2 from peripheral (70%–80%) to central (0%–5%) collisions. The centrality dependence is found to be similar to that observed at lower collision energies. The data are compared with models based on different mechanisms for particle production in nuclear collisions.

DOI: [10.1103/PhysRevLett.106.032301](https://doi.org/10.1103/PhysRevLett.106.032301)

PACS numbers: 25.75.Gz

Quantum chromodynamics (QCD), the theory of the strong interaction, predicts a phase transition at high temperature between hadronic and deconfined matter (the quark-gluon plasma). Strongly interacting matter under such extreme conditions can be studied experimentally using ultrarelativistic collisions of heavy nuclei. The field entered a new era in November 2010 when the Large Hadron Collider (LHC) at CERN produced the first Pb-Pb collisions at a center-of-mass energy per nucleon pair $\sqrt{s_{\text{NN}}} = 2.76$ TeV. This represents an increase of more than 1 order of magnitude over the highest energy nuclear collisions previously obtained in the laboratory.

The multiplicity of charged particles produced in the central rapidity region is a key observable to characterize the properties of the matter created in these collisions [1]. Nuclei are extended objects, and their collisions can be characterized by centrality, related to the collision impact parameter. The study of the dependence of the charged-particle density on colliding system, center-of-mass energy and collision geometry is important to understand the relative contributions to particle production of hard scattering and soft processes, and may provide insight into the partonic structure of the projectiles.

The ALICE Collaboration recently reported the measurement of the charged-particle pseudorapidity density at midrapidity for the most central (head-on) Pb-Pb collisions at $\sqrt{s_{\text{NN}}} = 2.76$ TeV [2]. In this Letter, we extend that study to noncentral collisions, presenting the measurement of the centrality dependence of the multiplicity density of charged primary particles $dN_{\text{ch}}/d\eta$ in the pseudorapidity interval $|\eta| < 0.5$. The pseudorapidity is defined as $\eta \equiv -\text{Intan}(\theta/2)$, where θ is the angle between the charged-particle direction and the beam axis (z). Primary particles

are defined as all prompt particles produced in the collision, including decay products, except those from weak decays of strange particles.

We report the charged-particle density per participant pair, $(dN_{\text{ch}}/d\eta)/(\langle N_{\text{part}} \rangle/2)$, for nine centrality classes, covering the most central 80% of the hadronic cross section. The average number of nucleons participating in the collision in a given centrality class, $\langle N_{\text{part}} \rangle$, reflects the collision geometry and is obtained using Glauber modeling [3]. The results are compared with measurements at lower collision energy [4–9] and with theoretical calculations [10–14].

The data for this measurement were collected with the ALICE detector [15]. The data sample is the same as in [2] and the analysis techniques are similar. The main detector utilized in the analysis is the silicon pixel detector (SPD), the innermost part of the inner tracking system (ITS). The SPD consists of two cylindrical layers of hybrid silicon pixel assemblies covering $|\eta| < 2.0$ and $|\eta| < 1.4$ for the inner and outer layers, respectively. A total of 9.8×10^6 pixels of size $50 \times 425 \mu\text{m}^2$ are read out by 1200 electronic chips. Each chip also provides a fast signal when at least one of its pixels is hit. These signals are combined in a programmable logic unit which supplies a trigger signal. A trigger signal is also provided by the VZERO counters, two arrays of 32 scintillator tiles covering the full azimuth within $2.8 < \eta < 5.1$ (VZERO-A) and $-3.7 < \eta < -1.7$ (VZERO-C). The trigger was configured for high efficiency for hadronic events, requiring at least two out of the following three conditions: (i) two pixel chips hit in the outer layer of the SPD, (ii) a signal in VZERO-A, (iii) a signal in VZERO-C. The threshold in the VZERO detector corresponds approximately to the energy deposition of a minimum ionizing particle. This trigger configuration led to a rate of about 50 Hz, with 4 Hz from nuclear interactions, 45 Hz from electromagnetic processes, and 1 Hz arising from beam background. In addition, in the offline event selection, we also use the information from two neutron zero degree calorimeters (ZDCs) positioned at ± 114 m from the interaction point. Beam background

*Full author list given at the end of the article.

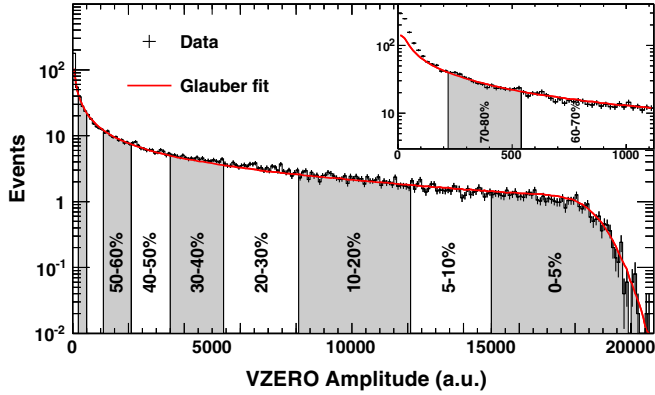


FIG. 1 (color online). Distribution of the summed amplitudes in the VZERO scintillator tiles (histogram); inset shows the low amplitude part of the distribution. The curve shows the result of the Glauber model fit to the measurement. The vertical lines separate the centrality classes used in the analysis, which in total correspond to the most central 80% of hadronic collisions.

events are removed using the VZERO and ZDC timing information. Electromagnetically induced interactions are reduced by requiring an energy deposition above 500 GeV in each of the neutron ZDCs.

After event selection, the sample consists of about blue 65 000 events. Figure 1 shows the distribution of the summed amplitudes in the VZERO scintillator tiles together with the distribution obtained with a model of particle production based on a Glauber description of nuclear collisions [3]. We use a two-component model assuming that the number of particle-producing sources is given by $f \times N_{\text{part}} + (1 - f) \times N_{\text{coll}}$, where N_{part} is the number of participating nucleons, N_{coll} is the number of binary nucleon-nucleon collisions and f quantifies their relative contributions. The number of particles produced by each source is distributed according to a negative binomial distribution, parametrized with μ and κ , where μ is the mean multiplicity per source and κ controls the large multiplicity tail.

In the Glauber calculation [16], the nuclear density for ^{208}Pb is modeled by a Woods-Saxon distribution for a spherical nucleus with a radius of 6.62 fm and a skin depth of 0.546 fm, based on data from low energy electron-nucleus scattering experiments [17]. A hard-sphere exclusion distance of 0.4 fm between nucleons is employed. Nuclear collisions are modeled by randomly displacing the two colliding nuclei in the transverse plane. Nucleons from each nucleus are assumed to collide if the transverse distance between them is less than the distance corresponding to the inelastic nucleon-nucleon cross section, estimated from interpolating data at different center-of-mass energies [18] to be 64 ± 5 mb at $\sqrt{s} = 2.76$ TeV

The values of f , μ , and κ are obtained from a fit to the measured VZERO amplitude distribution. The fit is restricted to amplitudes above a value corresponding to 88% of the hadronic cross section. In this region the trigger

and event selection are fully efficient, and the contamination by electromagnetic processes is negligible. Centrality classes are determined by integrating the measured distribution above the cut, as shown in Fig. 1.

The determination of $dN_{\text{ch}}/d\eta$ is performed for each centrality class. The primary vertex position is extracted by correlating hits in the two SPD layers. All events in the sample corresponding to 0%–80% of the hadronic cross section are found to have a well-defined primary vertex. To minimize edge effects at the limit of the SPD acceptance, we require $|z_{\text{vtx}}| < 7$ cm for the reconstructed vertex, leading to a sample of about 49 000 events.

The measurement of the charged-particle multiplicity is based on the reconstruction of tracklets [2]. A tracklet candidate is defined as a pair of hits, one in each SPD layer. Using the reconstructed vertex as the origin, differences in azimuthal ($\Delta\phi$, bending plane) and polar ($\Delta\theta$, nonbending direction) angles for pairs of hits are calculated [19]. Tracklets are defined by hit combinations that satisfy a selection on the sum of the squares (δ^2) of $\Delta\phi$ and $\Delta\theta$, each normalized to its estimated resolution (60 mrad for $\Delta\phi$ and $25\sin^2\theta$ m rad for $\Delta\theta$). The tolerance in $\Delta\phi$ for tracklet reconstruction effectively selects charged particles with transverse momentum above 50 MeV/ c . If multiple tracklet candidates share a hit, only the combination with the smallest δ^2 is kept.

The charged-particle pseudorapidity density $dN_{\text{ch}}/d\eta$ in $|\eta| < 0.5$ is obtained from the number of tracklets by applying a correction $\alpha \times (1 - \beta)$ in bins of pseudorapidity and z position of the primary vertex. The factor α corrects for the acceptance and efficiency of a primary track to form a tracklet, and β reflects the fraction of background tracklets from uncorrelated hits. The fraction β is estimated by matching the tails of the data and background δ^2 distributions. The latter is obtained by selecting combinatorial tracklets from a sample of simulated events with similar SPD hit multiplicities generated with HIJING [20] and a GEANT3 [21] model of the detector response. The estimated background fraction varies from 1% in the most peripheral to 14% in the most central class.

The correction α is obtained as the ratio of the number of generated primary charged particles and the number of reconstructed tracklets, after subtraction of the combinatorial background. Thus, α includes the corrections for the geometrical acceptance, detector and reconstruction inefficiencies, contamination by weak decay products of strange particles, photon conversions, secondary interactions, and undetected particles with transverse momentum below 50 MeV/ c . The correction is about 1.8 and varies little with centrality. Its magnitude is dominated by the effect of tracklet acceptance: the fraction of SPD channels active during data taking was 70% for the inner and 78% for the outer layer.

Systematic uncertainties on $dN_{\text{ch}}/d\eta$ are estimated as follows: for *background subtraction*, from 0.1% in the

most peripheral to 2.0% in the most central class, by using an alternative method where fake hits are injected into real events; for *particle composition*, 1%, by changing the relative abundances of protons, pions, kaons by up to a factor of 2; for contamination by weak decays, 1%, by changing the relative contribution of the yield of strange particles by a factor of 2; for extrapolation to zero transverse momentum, 2%, by varying the estimated yield of particles at low transverse momentum by a factor of 2; for dependence on event generator, 2%, by using quenched and unquenched versions of HIJING [20], as well as DPMJET [22] for calculating the corrections. The systematic uncertainty on $dN_{\text{ch}}/d\eta$ due to the centrality class definition is estimated as 6.2% for the most peripheral and 0.4% for the most central class, by using alternative centrality definitions based on track or SPD hit multiplicities, by using different ranges for the Glauber model fit, by defining cross-section classes integrating over the fit rather than directly over the data distributions, by changing the N_{part} dependence of the particle production model to a power law, and by changing the nucleon—nucleon cross section and the parameters of the Woods—Saxon distribution within their estimated uncertainties and by changing the internucleon exclusion distance by $\pm 100\%$. All other sources of systematic errors considered (tracklet cuts, vertex cuts, material budget, detector efficiency, background events) were found to be negligible. The total systematic uncertainty on $dN_{\text{ch}}/d\eta$ amounts to 7.0% in the most peripheral and 3.8% in the most central class. A large part of this uncertainty, about 5.0% for the most peripheral and 2.5% for the most central class, is correlated among the different centrality classes. The $dN_{\text{ch}}/d\eta$ values obtained for nine centrality classes together with their systematic uncertainties are given in Table I. As a cross check of the centrality selection the $dN_{\text{ch}}/d\eta$ analysis was repeated using centrality cuts defined by slicing perpendicularly to the correlation between the energy deposited in the ZDC and the VZERO amplitude. The resulting $dN_{\text{ch}}/d\eta$ values differ by 3.5% in the most peripheral (70%–80%) and by less than 2% in all the other classes from those obtained by

TABLE I. $dN_{\text{ch}}/d\eta$ and $(dN_{\text{ch}}/d\eta)/(\langle N_{\text{part}} \rangle/2)$ values measured in $|\eta| < 0.5$ for nine centrality classes. The $\langle N_{\text{part}} \rangle$ obtained with the Glauber model are given.

Centrality	$dN_{\text{ch}}/d\eta$	$\langle N_{\text{part}} \rangle$	$(dN_{\text{ch}}/d\eta)/(\langle N_{\text{part}} \rangle/2)$
0%–5%	1601 ± 60	382.8 ± 3.1	8.4 ± 0.3
5%–10%	1294 ± 49	329.7 ± 4.6	7.9 ± 0.3
10%–20%	966 ± 37	260.5 ± 4.4	7.4 ± 0.3
20%–30%	649 ± 23	186.4 ± 3.9	7.0 ± 0.3
30%–40%	426 ± 15	128.9 ± 3.3	6.6 ± 0.3
40%–50%	261 ± 9	85.0 ± 2.6	6.1 ± 0.3
50%–60%	149 ± 6	52.8 ± 2.0	5.7 ± 0.3
60%–70%	76 ± 4	30.0 ± 1.3	5.1 ± 0.3
70%–80%	35 ± 2	15.8 ± 0.6	4.4 ± 0.4

using the VZERO selection alone, which is well within the systematic uncertainty. Independent cross checks performed using tracks reconstructed in the TPC and ITS instead of tracklets yield compatible results.

In order to compare bulk particle production in different collision systems and at different energies, the charged-particle density is divided by the average number of participating nucleon pairs, $\langle N_{\text{part}} \rangle/2$, determined for each centrality class. The $\langle N_{\text{part}} \rangle$ values are obtained using the Glauber calculation, by classifying events according to the impact parameter, without reference to a specific particle production model, and are listed in Table I. The systematic uncertainty in the $\langle N_{\text{part}} \rangle$ values is obtained by varying the parameters entering the Glauber calculation as described above. The geometrical $\langle N_{\text{part}} \rangle$ values are consistent within uncertainties with the values extracted from the Glauber fit in each centrality class, and agree to better than 1% except for the 70–80% class where the difference is 3.5%.

Figure 2 presents $(dN_{\text{ch}}/d\eta)/(\langle N_{\text{part}} \rangle/2)$ as a function of the number of participants. Point-to-point, uncorrelated uncertainties are indicated by the error bars, while correlated uncertainties are shown as the grey band. Statistical errors are negligible. The charged-particle density per participant pair increases with $\langle N_{\text{part}} \rangle$, from 4.4 ± 0.4 for the most peripheral to 8.4 ± 0.3 for the most central class. The values for Au-Au collisions at $\sqrt{s_{\text{NN}}} = 0.2$ TeV, averaged over the RHIC experiments [7], are shown in the same

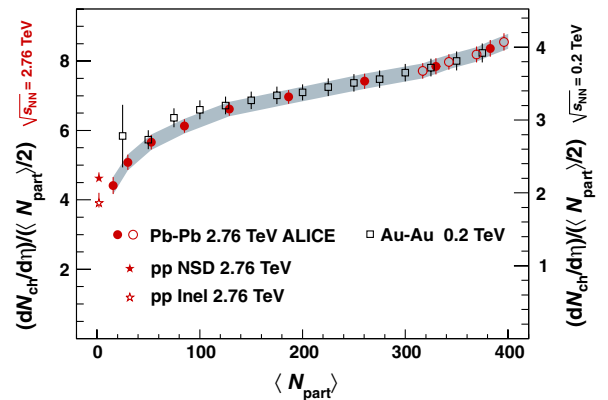


FIG. 2 (color online). Dependence of $(dN_{\text{ch}}/d\eta)/(\langle N_{\text{part}} \rangle/2)$ on the number of participants for Pb-Pb collisions at $\sqrt{s_{\text{NN}}} = 2.76$ TeV and Au-Au collisions at $\sqrt{s_{\text{NN}}} = 0.2$ TeV (RHIC average) [7]. The scale for the lower-energy data is shown on the right-hand side and differs from the scale for the higher-energy data on the left-hand side by a factor of 2.1. For the Pb-Pb data, uncorrelated uncertainties are indicated by the error bars, while correlated uncertainties are shown as the grey band. Statistical errors are negligible. The open circles show the values obtained for centrality classes obtained by dividing the 0%–10% most central collisions into four, rather than two classes. The values for non-single-diffractive and inelastic pp collisions are the results of interpolating between data at 2.36 [19,24] and 7 TeV [25].

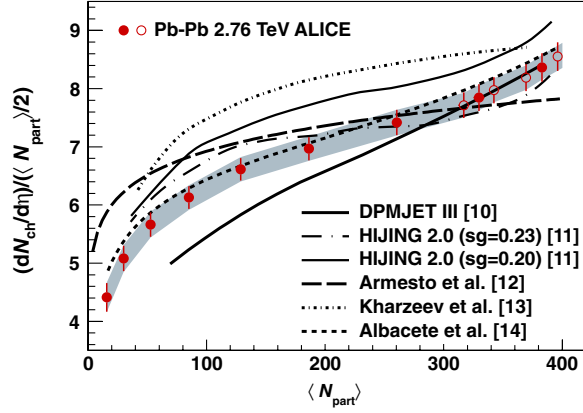


FIG. 3 (color online). Comparison of $(dN_{ch}/d\eta)/(\langle N_{part} \rangle/2)$ with model calculations for Pb-Pb at $\sqrt{s_{NN}} = 2.76$ TeV. Uncertainties in the data are shown as in Fig. 2. The HIJING 2.0 curve is shown for two values of the gluon shadowing (s_g) parameter.

figure with a scale that differs by a factor of 2.1 on the right-hand side. The centrality dependence of the multiplicity is found to be very similar for $\sqrt{s_{NN}} = 2.76$ TeV and $\sqrt{s_{NN}} = 0.2$ TeV.

Theoretical descriptions of particle production in nuclear collisions fall into two broad categories: two-component models combining perturbative QCD processes (e.g., jets and mini jets) with soft interactions, and saturation models with various parametrizations for the energy and centrality dependence of the saturation scale. In Fig. 3 we compare the measured $(N_{ch}/d\eta)/(\langle N_{part} \rangle/2)$ with model predictions. A calculation based on the two-component Dual Parton Model (DPMJET [10], with string fusion) exhibits a stronger rise with centrality than observed. The two-component HIJING 2.0 model [23], which has been tuned [11] (Published after the most central $dN_{ch}/d\eta$ value [2] was known.) to high-energy pp [19,24] and central Pb-Pb data [2], reasonably describes the data. This model includes a strong impact parameter dependent gluon shadowing (s_g) which limits the rise of particle production with centrality. The remaining models show a weak dependence of multiplicity on centrality. They are all different implementations of the saturation picture, where the number of soft gluons available for scattering and particle production is reduced by nonlinear interactions and parton recombination. A geometrical scaling model with a strong dependence of the saturation scale on nuclear mass and collision energy [12] predicts a rather weak variation with centrality. The centrality dependence is well reproduced by saturation models [13,14] (Published after the most central $dN_{ch}/d\eta$ value [2] was known.), although the former overpredicts the magnitude.

In summary, the measurement of the centrality dependence of the charged-particle multiplicity density at mid-rapidity in Pb-Pb collisions at $\sqrt{s_{NN}} = 2.76$ TeV has been presented. The charged-particle density normalized per

participating nucleon pair increases by about a factor 2 from peripheral (70%–80%) to central (0%–5%) collisions. The dependence of the multiplicity on centrality is strikingly similar for the data at $\sqrt{s_{NN}} = 2.76$ TeV and $\sqrt{s_{NN}} = 0.2$ TeV. Theoretical descriptions that include a moderation of the multiplicity evolution with centrality are favored by the data.

The ALICE collaboration would like to thank all its engineers and technicians for their invaluable contributions to the construction of the experiment and the CERN accelerator teams for the outstanding performance of the LHC complex. The ALICE collaboration acknowledges the following funding agencies for their support in building and running the ALICE detector: Calouste Gulbenkian Foundation from Lisbon and Swiss Fonds Kidagan, Armenia; Conselho Nacional de Desenvolvimento Científico e Tecnológico (CNPq), Financiadora de Estudos e Projetos (FINEP), Fundação de Amparo à Pesquisa do Estado de São Paulo (FAPESP); National Natural Science Foundation of China (NSFC), the Chinese Ministry of Education (CMOE) and the Ministry of Science and Technology of China (MSTC); Ministry of Education and Youth of the Czech Republic; Danish Natural Science Research Council, the Carlsberg Foundation and the Danish National Research Foundation; The European Research Council under the European Community’s Seventh Framework Programme; Helsinki Institute of Physics and the Academy of Finland; French CNRS-IN2P3, the “Region Pays de Loire”, “Region Alsace”, “Region Auvergne” and CEA, France; German BMBF and the Helmholtz Association; Greek Ministry of Research and Technology; Hungarian OTKA and National Office for Research and Technology (NKTH); Department of Atomic Energy and Department of Science and Technology of the Government of India; Istituto Nazionale di Fisica Nucleare (INFN) of Italy; MEXT Grant-in-Aid for Specially Promoted Research, Japan; Joint Institute for Nuclear Research, Dubna; National Research Foundation of Korea (NRF); CONACYT, DGAPA, México, ALFA-EC and the HELEN Program (High-Energy physics Latin-American–European Network); Stichting voor Fundamenteel Onderzoek der Materie (FOM) and the Nederlandse Organisatie voor Wetenschappelijk Onderzoek (NWO), Netherlands; Research Council of Norway (NFR); Polish Ministry of Science and Higher Education; National Authority for Scientific Research—NASR (Autoritatea Națională pentru Cercetare Științifică—ANCS); Federal Agency of Science of the Ministry of Education and Science of Russian Federation, International Science and Technology Center, Russian Academy of Sciences, Russian Federal Agency of Atomic Energy, Russian Federal Agency for Science and Innovations and CERN-INTAS; Ministry of Education of Slovakia; CIEMAT, EELA, Ministerio de Educación y Ciencia of Spain,

Xunta de Galicia (Consellería de Educación), CEADEN, Cubaenergía, Cuba, and IAEA (International Atomic Energy Agency); The Ministry of Science and Technology and the National Research Foundation (NRF), South Africa; Swedish Research Council (VR) and Knut & Alice Wallenberg Foundation (KAW); Ukraine Ministry of Education and Science; United Kingdom Science and Technology Facilities Council (STFC); The United States Department of Energy, the United States National Science Foundation, the State of Texas, and the State of Ohio.

- [1] N. Armesto, [arXiv:0903.1330](#).
- [2] K. Aamodt *et al.* (ALICE Collaboration), *Phys. Rev. Lett.* **105**, 252301 (2010).
- [3] M. L. Miller, K. Reygers, S. J. Sanders, and P. Steinberg, *Annu. Rev. Nucl. Part. Sci.* **57**, 205 (2007).
- [4] K. Adcox *et al.* (PHENIX Collaboration), *Phys. Rev. Lett.* **86**, 3500 (2001).
- [5] B. B. Back *et al.* (PHOBOS Collaboration), *Phys. Rev. C* **65**, 031901 (2002).
- [6] B. B. Back *et al.* (PHOBOS Collaboration), *Phys. Rev. C* **65**, 061901 (2002).
- [7] S. S. Adler *et al.* (PHENIX Collaboration), *Phys. Rev. C* **71**, 034908 (2005).
- [8] B. I. Abelev *et al.* (STAR Collaboration), *Phys. Rev. C* **79**, 034909 (2009).
- [9] B. Alver *et al.* (PHOBOS Collaboration), [arXiv:1011.1940](#).
- [10] F. Bopp, R. Engel, J. Ranft, and S. Roesler, [arXiv:0706.3875](#), interpolated between 2.0 and 5.5 TeV values.
- [11] W.-T. Deng, X.-N. Wang, and R. Xu, [arXiv:1011.5907](#).
- [12] N. Armesto, C. A. Salgado, and U. A. Wiedemann, *Phys. Rev. Lett.* **94**, 022002 (2005).
- [13] D. Kharzeev, E. Levin, and M. Nardi, *Nucl. Phys. A* **747**, 609 (2005).
- [14] J. L. Albacete and A. Dumitru, [arXiv:1011.5161](#).
- [15] K. Aamodt *et al.* (ALICE Collaboration), *JINST* **3**, S08002 (2008).
- [16] B. Alver, M. Baker, C. Loizides, and P. Steinberg, [arXiv:0805.4411](#).
- [17] H. De Vries, C. W. De Jager, and C. De Vries, *At. Data Nucl. Data Tables* **36**, 495 (1987). Since the Woods-Saxon parameters for ^{208}Pb are not available, we use the values for ^{207}Pb . Note that the Bessel-Fourier coefficients for the two nuclei are similar.
- [18] K. Nakamura *et al.* (Particle Data Group), *J. Phys. G* **37**, 075021 (2010).
- [19] K. Aamodt *et al.* (ALICE Collaboration), *Eur. Phys. J. C* **68**, 89 (2010).
- [20] X.-N. Wang and M. Gyulassy, *Phys. Rev. D* **44**, 3501 (1991).
- [21] R. Brun *et al.*, CERN Program Library Long Write-up, W5013, GEANT Detector Description and Simulation Tool (1994).
- [22] S. Roesler, R. Engel, and J. Ranft, [arXiv:hep-ph/0012252](#).
- [23] W.-T. Deng, X.-N. Wang, and R. Xu, [arXiv:1008.1841](#).
- [24] V. Khachatryan *et al.* (CMS Collaboration), *J. High Energy Phys.* **02** (2010) 041.
- [25] V. Khachatryan *et al.* (CMS Collaboration), *Phys. Rev. Lett.* **105**, 022002 (2010).
- K. Aamodt,¹ A. Abrahantes Quintana,² D. Adamová,³ A. M. Adare,⁴ M. M. Aggarwal,⁵ G. Aglieri Rinella,⁶ A. G. Agocs,⁷ S. Aguilar Salazar,⁸ Z. Ahammed,⁹ N. Ahmad,¹⁰ A. Ahmad Masoodi,¹⁰ S. U. Ahn,^{11,b} A. Akindinov,¹² D. Aleksandrov,¹³ B. Alessandro,¹⁴ R. Alfaro Molina,⁸ A. Alici,^{15,c} A. Alkin,¹⁶ E. Almaráz Aviña,⁸ T. Alt,¹⁷ V. Altini,^{18,d} S. Altinpinar,¹⁹ I. Altsybeev,²⁰ C. Andrei,²¹ A. Andronic,¹⁹ V. Anguelov,^{22,e} C. Anson,²³ T. Antičić,²⁴ F. Antinori,²⁵ P. Antonioli,²⁶ L. Aphecetche,²⁷ H. Appelshäuser,²⁸ N. Arbor,²⁹ S. Arcelli,¹⁵ A. Arend,²⁸ N. Armesto,³⁰ R. Arnaldi,¹⁴ T. Aronsson,⁴ I. C. Arsene,¹⁹ A. Asryan,²⁰ A. Augustinus,⁶ R. Averbeck,¹⁹ T. C. Awes,³¹ J. Äystö,³² M. D. Azmi,¹⁰ M. Bach,¹⁷ A. Badalà,³³ Y. W. Baek,^{11,b} S. Bagnasco,¹⁴ R. Bailhache,²⁸ R. Bala,^{34,f} R. Baldini Ferroli,³⁵ A. Baldisseri,³⁶ A. Baldit,³⁷ J. Bán,³⁸ R. Barbera,³⁹ F. Barile,¹⁸ G. G. Barnaföldi,⁷ L. S. Barnby,⁴⁰ V. Barret,³⁷ J. Bartke,⁴¹ M. Basile,¹⁵ N. Bastid,³⁷ B. Bathen,⁴² G. Batigne,²⁷ B. Batyunya,⁴³ C. Baumann,²⁸ I. G. Bearden,⁴⁴ H. Beck,²⁸ I. Belikov,⁴⁵ F. Bellini,¹⁵ R. Bellwied,^{46,g} E. Belmont-Moreno,⁸ S. Beole,³⁴ I. Berceanu,²¹ A. Bercuci,²¹ E. Berdermann,¹⁹ Y. Berdnikov,⁴⁷ L. Betev,⁶ A. Bhasin,⁴⁸ A. K. Bhati,⁵ L. Bianchi,³⁴ N. Bianchi,⁴⁹ C. Bianchin,⁵⁰ J. Bielčik,⁵¹ J. Bielčíková,³ A. Bilandzic,⁵² E. Biolcati,^{6,h} A. Blanc,³⁷ F. Blanco,⁵³ F. Blanco,⁵⁴ D. Blau,¹³ C. Blume,²⁸ M. Boccioni,⁶ N. Bock,²³ A. Bogdanov,⁵⁵ H. Bøggild,⁴⁴ M. Bogolyubsky,⁵⁶ L. Boldizsár,⁷ M. Bombara,⁵⁷ C. Bombonati,⁵⁰ J. Book,²⁸ H. Borel,³⁶ C. Bortolin,^{50,i} S. Bose,⁵⁸ F. Bossú,^{6,h} M. Botje,⁵² S. Böttger,²² B. Boyer,⁵⁹ P. Braun-Munzinger,¹⁹ L. Bravina,⁶⁰ M. Bregant,^{61,j} T. Breitner,²² M. Broz,⁶² R. Brun,⁶ E. Bruna,⁴ G. E. Bruno,¹⁸ D. Budnikov,⁶³ H. Buesching,²⁸ O. Busch,⁶⁴ Z. Buthelezi,⁶⁵ D. Caffarri,⁵⁰ X. Cai,⁶⁶ H. Caines,⁴ E. Calvo Villar,⁶⁷ P. Camerini,⁶¹ V. Canoa Roman,^{6,k} G. Cara Romeo,²⁶ F. Carena,⁶ W. Carena,⁶ F. Carminati,⁶ A. Casanova Díaz,⁴⁹ M. Caselle,⁶ J. Castillo Castellanos,³⁶ V. Catanescu,²¹ C. Cavicchioli,⁶ P. Cerello,¹⁴ B. Chang,³² S. Chapeland,⁶ J. L. Charvet,³⁶ S. Chattopadhyay,⁵⁸ S. Chattopadhyay,⁹ M. Cherney,⁶⁸ C. Cheshkov,⁶⁹ B. Cheynis,⁶⁹ E. Chiavassa,¹⁴ V. Chibante Barroso,⁶ D. D. Chinellato,⁷⁰ P. Chochula,⁶ M. Chojnacki,⁷¹ P. Christakoglou,⁷¹ C. H. Christensen,⁴⁴ P. Christiansen,⁷² T. Chujo,⁷³ C. Cicalo,⁷⁴ L. Cifarelli,¹⁵ F. Cindolo,²⁶ J. Cleymans,⁶⁵ F. Coccetti,³⁵ J.-P. Coffin,⁴⁵ S. Coli,¹⁴ G. Conesa Balbastre,^{49,l} Z. Conesa del Valle,^{27,m}

- P. Constantin,⁶⁴ G. Contin,⁶¹ J. G. Contreras,⁷⁵ T. M. Cormier,⁴⁶ Y. Corrales Morales,³⁴ I. Cortés Maldonado,⁷⁶ P. Cortese,⁷⁷ M. R. Cosentino,⁷⁰ F. Costa,⁶ M. E. Cotallo,⁵³ E. Crescio,⁷⁵ P. Crochet,³⁷ E. Cuautle,⁷⁸ L. Cunqueiro,⁴⁹ G. D. Erasmo,¹⁸ A. Dainese,^{79,n} H. H. Dalsgaard,⁴⁴ A. Danu,⁸⁰ D. Das,⁵⁸ I. Das,⁵⁸ A. Dash,⁸¹ S. Dash,¹⁴ S. De,⁹ A. De Azevedo Moregula,⁴⁹ G. O. V. de Barros,⁸² A. De Caro,⁸³ G. de Cataldo,⁸⁴ J. de Cuveland,¹⁷ A. De Falco,⁸⁵ D. De Gruttola,⁸³ N. De Marco,¹⁴ S. De Pasquale,⁸³ R. De Remigis,¹⁴ R. de Rooij,⁷¹ H. Delagrangé,²⁷ Y. Delgado Mercado,⁶⁷ G. Dellacasa,^{77,a} A. Deloff,⁸⁶ V. Demanov,⁶³ E. Dénes,⁷ A. Deppman,⁸² D. Di Bari,¹⁸ C. Di Giglio,¹⁸ S. Di Liberto,⁸⁷ A. Di Mauro,⁶ P. Di Nezza,⁴⁹ T. Dietel,⁴² R. Divià,⁶ Ø. Djuvsland,¹ A. Dobrin,^{46,o} T. Dobrowolski,⁸⁶ I. Domínguez,⁷⁸ B. Dönigus,¹⁹ O. Dordic,⁶⁰ O. Driga,²⁷ A. K. Dubey,⁹ L. Ducroux,⁶⁹ P. Dupieux,³⁷ A. K. Dutta Majumdar,⁵⁸ M. R. Dutta Majumdar,⁹ D. Elia,⁸⁴ D. Emschermann,⁴² H. Engel,²² H. A. Erdal,⁸⁸ B. Espagnon,⁵⁹ M. Estienne,²⁷ S. Esumi,⁷³ D. Evans,⁴⁰ S. Evrard,⁶ G. Eyyubova,⁶⁰ C. W. Fabjan,^{6,p} D. Fabris,²⁵ J. Faivre,²⁹ D. Falchieri,¹⁵ A. Fantoni,⁴⁹ M. Fasel,¹⁹ R. Fearick,⁶⁵ A. Fedunov,⁴³ D. Fehlker,¹ V. Fekete,⁶² D. Felea,⁸⁰ G. Feofilov,²⁰ A. Fernández Téllez,⁷⁶ A. Ferretti,³⁴ R. Ferretti,^{77,d} M. A. S. Figueredo,⁸² S. Filchagin,⁶³ R. Fini,⁸⁴ D. Finogeev,⁸⁹ F. M. Fionda,¹⁸ E. M. Fiore,¹⁸ M. Floris,⁶ S. Foertsch,⁶⁵ P. Foka,¹⁹ S. Fokin,¹³ E. Fragiaco,⁹⁰ M. Fragkiadakis,⁹¹ U. Frankenfeld,¹⁹ U. Fuchs,⁶ F. Furano,⁶ C. Furget,²⁹ M. Fusco Girard,⁸³ J. J. Gaardhøje,⁴⁴ S. Gadrat,²⁹ M. Gagliardi,³⁴ A. Gago,⁶⁷ M. Gallio,³⁴ P. Ganoti,^{91,q} C. Garabatos,¹⁹ R. Gemme,⁷⁷ J. Gerhard,¹⁷ M. Germain,²⁷ C. Geuna,³⁶ A. Gheata,⁶ M. Gheata,⁶ B. Ghidini,¹⁸ P. Ghosh,⁹ M. R. Girard,⁹² G. Giraudo,¹⁴ P. Giubellino,^{34,r} E. Gladysz-Dziadus,⁴¹ P. Glässel,⁶⁴ R. Gomez,⁹³ L. H. González-Trueba,⁸ P. González-Zamora,⁵³ H. González Santos,⁷⁶ S. Gorbunov,¹⁷ S. Gotovac,⁹⁴ V. Grabski,⁸ R. Grajcarek,⁶⁴ A. Grelli,⁷¹ A. Grigoras,⁶ C. Grigoras,⁶ V. Grigoriev,⁵⁵ A. Grigoryan,⁹⁵ S. Grigoryan,⁴³ B. Grinyov,¹⁶ N. Grion,⁹⁰ P. Gros,⁷² J. F. Grosse-Oetringhaus,⁶ J.-Y. Grossiord,⁶⁹ R. Grosso,²⁵ F. Guber,⁸⁹ R. Guernane,²⁹ C. Guerra Gutierrez,⁶⁷ B. Guerzoni,¹⁵ K. Gulbrandsen,⁴⁴ H. Gulkanyan,⁹⁵ T. Gunji,⁹⁶ A. Gupta,⁴⁸ R. Gupta,⁴⁸ H. Gutbrod,¹⁹ Ø. Haaland,¹ C. Hadjidakis,⁵⁹ M. Haiduc,⁸⁰ H. Hamagaki,⁹⁶ G. Hamar,⁷ J. W. Harris,⁴ M. Hartig,²⁸ D. Hasch,⁴⁹ D. Hasegan,⁸⁰ D. Hatzifotiadou,²⁶ A. Hayrapetyan,^{95,d} M. Heide,⁴² M. Heinz,⁴ H. Helstrup,⁸⁸ A. Hergelegiu,²¹ C. Hernández,¹⁹ G. Herrera Corral,⁷⁵ N. Herrmann,⁶⁴ K. F. Hetland,⁸⁸ B. Hicks,⁴ P. T. Hille,⁴ B. Hippolyte,⁴⁵ T. Horaguchi,⁷³ Y. Hori,⁹⁶ P. Hristov,⁶ I. Hřivnáčová,⁵⁹ M. Huang,¹ S. Huber,¹⁹ T. J. Humanic,²³ D. S. Hwang,⁹⁷ R. Ichou,²⁷ R. Ilkaev,⁶³ I. Ilkiv,⁸⁶ M. Inaba,⁷³ E. Incani,⁸⁵ G. M. Innocenti,³⁴ P. G. Innocenti,⁶ M. Ippolitov,¹³ M. Irfan,¹⁰ C. Ivan,¹⁹ A. Ivanov,²⁰ M. Ivanov,¹⁹ V. Ivanov,⁴⁷ A. Jachoňkowski,⁶ P. M. Jacobs,⁹⁸ L. Jancurová,⁴³ S. Jangal,⁴⁵ R. Janik,⁶² S. P. Jayarathna,^{54,s} S. Jena,⁹⁹ L. Jirdeň,⁶ G. T. Jones,⁴⁰ P. G. Jones,⁴⁰ P. Jovanović,⁴⁰ H. Jung,¹¹ W. Jung,¹¹ A. Jusko,⁴⁰ S. Kalcher,¹⁷ P. Kaliňák,³⁸ M. Kalisky,⁴² T. Kalliokoski,³² A. Kalweit,¹⁰⁰ R. Kamermans,^{71,a} K. Kanaki,¹ E. Kang,¹¹ J. H. Kang,¹⁰¹ V. Kaplin,⁵⁵ O. Karavichev,⁸⁹ T. Karavicheva,⁸⁹ E. Karpechev,⁸⁹ A. Kazantsev,¹³ U. Kebschull,²² R. Keidel,¹⁰² M. M. Khan,¹⁰ A. Khanzadeev,⁴⁷ Y. Kharlov,⁵⁶ B. Kileng,⁸⁸ D. J. Kim,³² D. S. Kim,¹¹ D. W. Kim,¹¹ H. N. Kim,¹¹ J. H. Kim,⁹⁷ J. S. Kim,¹¹ M. Kim,¹¹ M. Kim,¹⁰¹ S. Kim,⁹⁷ S. H. Kim,¹¹ S. Kirsch,^{6,t} I. Kisel,^{22,u} S. Kiselev,¹² A. Kisiel,⁶ J. L. Klay,¹⁰³ J. Klein,⁶⁴ C. Klein-Bösing,⁴² M. Kliemant,²⁸ A. Klovning,¹ A. Kluge,⁶ M. L. Knichel,¹⁹ K. Koch,⁶⁴ M. K. Köhler,¹⁹ R. Kolevatov,⁶⁰ A. Kolojvari,²⁰ V. Kondratiev,²⁰ N. Kondratyeva,⁵⁵ A. Konevskih,⁸⁹ E. Kornać,⁴¹ C. Kottachchi Kankanamge Don,⁴⁶ R. Kour,⁴⁰ M. Kowalski,⁴¹ S. Kox,²⁹ G. Koyithatta Meethalevedu,⁹⁹ K. Kozlov,¹³ J. Kral,³² I. Králik,³⁸ F. Kramer,²⁸ I. Kraus,^{100,v} T. Krawutschke,^{64,w} M. Kretz,¹⁷ M. Krivda,^{40,x} D. Krumbhorn,⁶⁴ M. Krus,⁵¹ E. Kryshen,⁴⁷ M. Krzewicki,⁵² Y. Kucheriaev,¹³ C. Kuhn,⁴⁵ P. G. Kuijer,⁵² P. Kurashvili,⁸⁶ A. Kurepin,⁸⁹ A. B. Kurepin,⁸⁹ A. Kuryakin,⁶³ S. Kushpil,³ V. Kushpil,³ M. J. Kweon,⁶⁴ Y. Kwon,¹⁰¹ P. La Rocca,³⁹ P. Ladrón de Guevara,^{53,y} V. Lafage,⁵⁹ C. Lara,²² D. T. Larsen,¹ C. Lazzeroni,⁴⁰ Y. Le Bornec,⁵⁹ R. Lea,⁶¹ K. S. Lee,¹¹ S. C. Lee,¹¹ F. Lefèvre,²⁷ J. Lehnert,²⁸ L. Leistam,⁶ M. Lenhardt,²⁷ V. Lenti,⁸⁴ I. León Monzón,⁹³ H. León Vargas,²⁸ P. Lévai,⁷ X. Li,¹⁰⁴ R. Lietava,⁴⁰ S. Lindal,⁶⁰ V. Lindenstruth,^{22,u} C. Lippmann,^{6,v} M. A. Lisa,²³ L. Liu,¹ V. R. Loggins,⁴⁶ V. Loginov,⁵⁵ S. Lohn,⁶ D. Lohner,⁶⁴ C. Loizides,⁹⁸ X. Lopez,³⁷ M. López Noriega,⁵⁹ E. López Torres,² G. Løvnhøiden,⁶⁰ X.-G. Lu,⁶⁴ P. Luettig,²⁸ M. Lunardon,⁵⁰ G. Luparello,³⁴ L. Luquin,²⁷ C. Luzzi,⁶ K. Ma,⁶⁶ R. Ma,⁴ D. M. Madagodahettige-Don,⁵⁴ A. Maevskaya,⁸⁹ M. Mager,⁶ D. P. Mahapatra,⁸¹ A. Maire,⁴⁵ M. Malaev,⁴⁷ I. Maldonado Cervantes,⁷⁸ D. Mal'Kevich,¹² P. Malzacher,¹⁹ A. Mamonov,⁶³ L. Manceau,³⁷ L. Mangotra,⁴⁸ V. Manko,¹³ F. Manso,³⁷ V. Manzari,⁸⁴ Y. Mao,^{66,z} J. Mareš,¹⁰⁵ G. V. Margagliotti,⁶¹ A. Margotti,²⁶ A. Marín,¹⁹ I. Martashvili,¹⁰⁶ P. Martinengo,⁶ M. I. Martínez,⁷⁶ A. Martínez Davalos,⁸ G. Martínez García,²⁷ Y. Martynov,¹⁶ A. Mas,²⁷ S. Masciocchi,¹⁹ M. Masera,³⁴ A. Masoni,⁷⁴ L. Massacrier,⁶⁹ M. Mastromarco,⁸⁴ A. Mastroserio,⁶ Z. L. Matthews,⁴⁰ A. Matyja,^{41,j} D. Mayani,⁷⁸ G. Mazza,¹⁴ M. A. Mazzoni,⁸⁷ F. Meddi,¹⁰⁷ A. Menchaca-Rocha,⁸ P. Mendez Lorenzo,⁶ J. Mercado Pérez,⁶⁴ P. Mereu,¹⁴ Y. Miake,⁷³ J. Midori,¹⁰⁸ L. Milano,³⁴ J. Milosevic,^{60,aa}

A. Mischke,⁷¹ D. Miśkowiec,^{19,r} C. Mitu,⁸⁰ J. Mlynarz,⁴⁶ B. Mohanty,⁹ L. Molnar,⁶ L. Montaño Zetina,⁷⁵ M. Monteno,¹⁴ E. Montes,⁵³ M. Morando,⁵⁰ D. A. Moreira De Godoy,⁸² S. Moretto,⁵⁰ A. Morsch,⁶ V. Muccifora,⁴⁹ E. Mudnic,⁹⁴ H. Müller,⁶ S. Muhuri,⁹ M. G. Munhoz,⁸² J. Munoz,⁷⁶ L. Musa,⁶ A. Musso,¹⁴ B. K. Nandi,⁹⁹ R. Nania,²⁶ E. Nappi,⁸⁴ C. Nattress,¹⁰⁶ F. Navach,¹⁸ S. Navin,⁴⁰ T. K. Nayak,⁹ S. Nazarenko,⁶³ G. Nazarov,⁶³ A. Nedosekin,¹² F. Nendaz,⁶⁹ J. Newby,¹⁰⁹ M. Nicassio,¹⁸ B. S. Nielsen,⁴⁴ S. Nikolaev,¹³ V. Nikolic,²⁴ S. Nikulin,¹³ V. Nikulin,⁴⁷ B. S. Nilsen,⁶⁸ M. S. Nilsson,⁶⁰ F. Noferini,²⁶ G. Nooren,⁷¹ N. Novitzky,³² A. Nyanin,¹³ A. Nyatha,⁹⁹ C. Nygaard,⁴⁴ J. Nystrand,¹ H. Obayashi,¹⁰⁸ A. Ochirov,²⁰ H. Oeschler,¹⁰⁰ S. K. Oh,¹¹ J. Oleniacz,⁹² C. Oppedisano,¹⁴ A. Ortiz Velasquez,⁷⁸ G. Ortona,^{6,h} A. Oskarsson,⁷² P. Ostrowski,⁹² I. Otterlund,⁷² J. Otwinowski,¹⁹ G. Øvrebekk,¹ K. Oyama,⁶⁴ K. Ozawa,⁹⁶ Y. Pachmayer,⁶⁴ M. Pachr,⁵¹ F. Padilla,³⁴ P. Pagano,^{6,bb} G. Paic,⁷⁸ F. Painke,¹⁷ C. Pajares,³⁰ S. Pal,³⁶ S. K. Pal,⁹ A. Palaha,⁴⁰ A. Palmeri,³³ G. S. Pappalardo,³³ W. J. Park,¹⁹ V. Paticchio,⁸⁴ A. Pavlinov,⁴⁶ T. Pawlak,⁹² T. Peitzmann,⁷¹ D. Peresunko,¹³ C. E. Pérez Lara,⁵² D. Perini,⁶ D. Perrino,¹⁸ W. Peryt,⁹² A. Pesci,²⁶ V. Peskov,^{6,cc} Y. Pestov,¹¹⁰ A. J. Peters,⁶ V. Petráček,⁵¹ M. Petris,²¹ P. Petrov,⁴⁰ M. Petrovici,²¹ C. Petta,³⁹ S. Piano,⁹⁰ A. Piccotti,¹⁴ M. Pikna,⁶² P. Pillot,²⁷ O. Pinazza,⁶ L. Pinsky,⁵⁴ N. Pitz,²⁸ F. Piuze,⁶ D. B. Piyarathna,^{46,dd} R. Platt,⁴⁰ M. Płoskoń,⁹⁸ J. Pluta,⁹² T. Pocheptsov,^{43,ee} S. Pochybova,⁷ P. L. M. Podesta-Lerma,⁹³ M. G. Poghosyan,³⁴ K. Polák,¹⁰⁵ B. Polichtchouk,⁵⁶ A. Pop,²¹ V. Pospíšil,⁵¹ B. Potukuchi,⁴⁸ S. K. Prasad,⁴⁶ R. Preghenella,³⁵ F. Prino,¹⁴ C. A. Pruneau,⁴⁶ I. Pshenichnov,⁸⁹ G. Puddu,⁸⁵ A. Pulvirenti,^{39,d} V. Punin,⁶³ M. Putiš,⁵⁷ J. Putschke,⁴ E. Quercigh,⁶ H. Qvigstad,⁶⁰ A. Rachevski,⁹⁰ A. Rademakers,⁶ O. Rademakers,⁶ S. Radomski,⁶⁴ T. S. Rähä,³² J. Rak,³² A. Rakotozafindrabe,³⁶ L. Ramello,⁷⁷ A. Ramírez Reyes,⁷⁵ M. Rammner,⁴² R. Raniwala,¹¹¹ S. Raniwala,¹¹¹ S. S. Räsänen,³² K. F. Read,¹⁰⁶ J. S. Real,²⁹ K. Redlich,⁸⁶ R. Renfordt,²⁸ A. R. Reolon,⁴⁹ A. Reshetin,⁸⁹ F. Rettig,¹⁷ J.-P. Revol,⁶ K. Reygers,⁶⁴ H. Ricaud,¹⁰⁰ L. Riccati,¹⁴ R. A. Ricci,⁷⁹ M. Richter,^{1,ff} P. Riedler,⁶ W. Riegler,⁶ F. Riggi,³⁹ A. Rivetti,¹⁴ M. Rodríguez Cahuantzi,⁷⁶ D. Rohr,¹⁷ D. Röhrich,¹ R. Romita,¹⁹ F. Ronchetti,⁴⁹ P. Rosinský,⁶ P. Rosnet,³⁷ S. Rossegger,⁶ A. Rossi,⁵⁰ F. Roukoutakis,⁹¹ S. Rousseau,⁵⁹ C. Roy,^{27,m} P. Roy,⁵⁸ A. J. Rubio Montero,⁵³ R. Rui,⁶¹ I. Rusanov,⁶ E. Ryabinkin,¹³ A. Rybicki,⁴¹ S. Sadovsky,⁵⁶ K. Šafařík,⁶ R. Sahoo,⁵⁰ P. K. Sahu,⁸¹ P. Saiz,⁶ S. Sakai,⁹⁸ D. Sakata,⁷³ C. A. Salgado,³⁰ T. Samanta,⁹ S. Sambyal,⁴⁸ V. Samsonov,⁴⁷ L. Šándor,³⁸ A. Sandoval,⁸ M. Sano,⁷³ S. Sano,⁹⁶ R. Santo,⁴² R. Santoro,⁸⁴ J. Sarkamo,³² P. Saturnini,³⁷ E. Scapparone,²⁶ F. Scarlassara,⁵⁰ R. P. Scharenberg,¹¹² C. Schiaua,²¹ R. Schicker,⁶⁴ C. Schmidt,¹⁹ H. R. Schmidt,^{19,gg} S. Schreiner,⁶ S. Schuchmann,²⁸ J. Schukraft,⁶ Y. Schutz,^{27,d} K. Schwarz,¹⁹ K. Schweda,⁶⁴ G. Scioli,¹⁵ E. Scomparin,¹⁴ P. A. Scott,⁴⁰ R. Scott,¹⁰⁶ G. Segato,⁵⁰ S. Senyukov,⁷⁷ J. Seo,¹¹ S. Serchi,⁸⁵ E. Serradilla,⁵³ A. Sevcenco,⁸⁰ G. Shabratova,⁴³ R. Shahoyan,⁶ N. Sharma,⁵ S. Sharma,⁴⁸ K. Shigaki,¹⁰⁸ M. Shimomura,⁷³ K. Shtejer,² Y. Sibiriak,¹³ M. Siciliano,³⁴ E. Sicking,⁶ T. Siemiarczuk,⁸⁶ A. Silenzi,¹⁵ D. Silvermyr,³¹ G. Simonetti,^{6,hh} R. Singaraju,⁹ R. Singh,⁴⁸ B. C. Sinha,⁹ T. Sinha,⁵⁸ B. Sitar,⁶² M. Sitta,⁷⁷ T. B. Skaali,⁶⁰ K. Skjerdal,¹ R. Smakal,⁵¹ N. Smirnov,⁴ R. Snellings,^{52,ii} C. Sjøgaard,⁴⁴ A. Soloviev,⁵⁶ R. Soltz,¹⁰⁹ H. Son,⁹⁷ M. Song,¹⁰¹ C. Soos,⁶ F. Soramel,⁵⁰ M. Spyropoulou-Stassinaki,⁹¹ B. K. Srivastava,¹¹² J. Stachel,⁶⁴ I. Stan,⁸⁰ G. Stefanek,⁸⁶ G. Stefanini,⁶ T. Steinbeck,^{22,u} E. Stenlund,⁷² G. Steyn,⁶⁵ D. Stocco,²⁷ R. Stock,²⁸ M. Stolpovskiy,⁵⁶ P. Strmen,⁶² A. A. P. Suaide,⁸² M. A. Subieta Vásquez,³⁴ T. Sugitate,¹⁰⁸ C. Suire,⁵⁹ M. Šumbera,³ T. Susa,²⁴ D. Swoboda,⁶ T. J. M. Symons,⁹⁸ A. Szanto de Toledo,⁸² I. Szarka,⁶² A. Szostak,¹ C. Tagridis,⁹¹ J. Takahashi,⁷⁰ J. D. Tapia Takaki,⁵⁹ A. Tauro,⁶ M. Tavlet,⁶ G. Tejada Muñoz,⁷⁶ A. Telesca,⁶ C. Terrevoli,¹⁸ J. Thäder,¹⁹ D. Thomas,⁷¹ J. H. Thomas,¹⁹ R. Tieulent,⁶⁹ A. R. Timmins,^{46,g} D. Tlusty,⁵¹ A. Toia,⁶ H. Torii,¹⁰⁸ L. Toscano,⁶ F. Tosello,¹⁴ T. Traczyk,⁹² D. Truesdale,²³ W. H. Trzaska,³² A. Tumkin,⁶³ R. Turrisi,²⁵ A. J. Turvey,⁶⁸ T. S. Tveter,⁶⁰ J. Ulery,²⁸ K. Ullaland,¹ A. Uras,⁸⁵ J. Urbán,⁵⁷ G. M. Urciuoli,⁸⁷ G. L. Usai,⁸⁵ A. Vacchi,⁹⁰ M. Vala,^{43,x} L. Valencia Palomo,⁵⁹ S. Vallero,⁶⁴ N. van der Kolk,⁵² M. van Leeuwen,⁷¹ P. Vande Vyvre,⁶ L. Vannucci,⁷⁹ A. Vargas,⁷⁶ R. Varma,⁹⁹ M. Vasileiou,⁹¹ A. Vasiliev,¹³ V. Vechernin,²⁰ M. Venaruzzo,⁶¹ E. Vercellin,³⁴ S. Vergara,⁷⁶ R. Vernet,¹¹³ M. Verweij,⁷¹ L. Vickovic,⁹⁴ G. Viesti,⁵⁰ O. Vikhlyantsev,⁶³ Z. Vilakazi,⁶⁵ O. Villalobos Baillie,⁴⁰ A. Vinogradov,¹³ L. Vinogradov,²⁰ Y. Vinogradov,⁶³ T. Virgili,⁸³ Y. P. Viyogi,⁹ A. Vodopyanov,⁴³ K. Voloshin,¹² S. Voloshin,⁴⁶ G. Volpe,¹⁸ B. von Haller,⁶ D. Vranic,¹⁹ J. Vrláková,⁵⁷ B. Vulpescu,³⁷ B. Wagner,¹ V. Wagner,⁵¹ R. Wan,^{45,jj} D. Wang,⁶⁶ Y. Wang,⁶⁴ Y. Wang,⁶⁶ K. Watanabe,⁷³ J. P. Wessels,⁴² U. Westerhoff,⁴² J. Wiechula,^{64,gg} J. Wikne,⁶⁰ M. Wilde,⁴² A. Wilk,⁴² G. Wilk,⁸⁶ M. C. S. Williams,²⁶ B. Windelband,⁶⁴ H. Yang,³⁶ S. Yasnopolskiy,¹³ J. Yi,¹¹⁴ Z. Yin,⁶⁶ H. Yokoyama,⁷³ I.-K. Yoo,¹¹⁴ X. Yuan,⁶⁶ I. Yushmanov,¹³ E. Zabrodin,⁶⁰ C. Zampolli,⁶ S. Zaporozhets,⁴³ A. Zarochentsev,²⁰ P. Závada,¹⁰⁵ H. Zbroszczyk,⁹² P. Zelnicek,²² A. Zenin,⁵⁶ I. Zgura,⁸⁰ M. Zhalov,⁴⁷ X. Zhang,^{66,b} D. Zhou,⁶⁶ X. Zhu,⁶⁶ A. Zichichi,^{15,kk} G. Zinovjev,¹⁶ Y. Zoccarato,⁶⁹ and M. Zynovev¹⁶

(ALICE Collaboration)

- ¹Department of Physics and Technology, University of Bergen, Bergen, Norway
²Centro de Aplicaciones Tecnológicas y Desarrollo Nuclear (CEADEN), Havana, Cuba
³Nuclear Physics Institute, Academy of Sciences of the Czech Republic, Řež u Prahy, Czech Republic
⁴Yale University, New Haven, Connecticut, United States
⁵Physics Department, Panjab University, Chandigarh, India
⁶European Organization for Nuclear Research (CERN), Geneva, Switzerland
⁷KFKI Research Institute for Particle and Nuclear Physics, Hungarian Academy of Sciences, Budapest, Hungary
⁸Instituto de Física, Universidad Nacional Autónoma de México, Mexico City, Mexico
⁹Variable Energy Cyclotron Centre, Kolkata, India
¹⁰Department of Physics Aligarh Muslim University, Aligarh, India
¹¹Gangneung-Wonju National University, Gangneung, South Korea
¹²Institute for Theoretical and Experimental Physics, Moscow, Russia
¹³Russian Research Centre Kurchatov Institute, Moscow, Russia
¹⁴Sezione INFN, Turin, Italy
¹⁵Dipartimento di Fisica dell'Università and Sezione INFN, Bologna, Italy
¹⁶Bogolyubov Institute for Theoretical Physics, Kiev, Ukraine
¹⁷Frankfurt Institute for Advanced Studies, Johann Wolfgang Goethe-Universität Frankfurt, Frankfurt, Germany
¹⁸Dipartimento Interateneo di Fisica 'M. Merlin' and Sezione INFN, Bari, Italy
¹⁹Research Division and ExtreMe Matter Institute EMMI, GSI Helmholtzzentrum für Schwerionenforschung, Darmstadt, Germany
²⁰V. Fock Institute for Physics, St. Petersburg State University, St. Petersburg, Russia
²¹National Institute for Physics and Nuclear Engineering, Bucharest, Romania
²²Kirchhoff-Institut für Physik, Ruprecht-Karls-Universität Heidelberg, Heidelberg, Germany
²³Department of Physics, Ohio State University, Columbus, Ohio, United States
²⁴Rudjer Bošković Institute, Zagreb, Croatia
²⁵Sezione INFN, Padova, Italy
²⁶Sezione INFN, Bologna, Italy
²⁷SUBATECH, Ecole des Mines de Nantes, Université de Nantes, CNRS-IN2P3, Nantes, France
²⁸Institut für Kernphysik, Johann Wolfgang Goethe-Universität Frankfurt, Frankfurt, Germany
²⁹Laboratoire de Physique Subatomique et de Cosmologie (LPSC), Université Joseph Fourier, CNRS-IN2P3, Institut Polytechnique de Grenoble, Grenoble, France
³⁰Departamento de Física de Partículas and IGFAE, Universidad de Santiago de Compostela, Santiago de Compostela, Spain
³¹Oak Ridge National Laboratory, Oak Ridge, Tennessee, United States
³²Helsinki Institute of Physics (HIP) and University of Jyväskylä, Jyväskylä, Finland
³³Sezione INFN, Catania, Italy
³⁴Dipartimento di Fisica Sperimentale dell'Università and Sezione INFN, Turin, Italy
³⁵Centro Fermi-Centro Studi e Ricerche e Museo Storico della Fisica "Enrico Fermi", Rome, Italy
³⁶Commissariat à l'Énergie Atomique, IRFU, Saclay, France
³⁷Laboratoire de Physique Corpusculaire (LPC), Clermont Université, Université Blaise Pascal, CNRS-IN2P3, Clermont-Ferrand, France
³⁸Institute of Experimental Physics, Slovak Academy of Sciences, Košice, Slovakia
³⁹Dipartimento di Fisica e Astronomia dell'Università and Sezione INFN, Catania, Italy
⁴⁰School of Physics and Astronomy, University of Birmingham, Birmingham, United Kingdom
⁴¹The Henryk Niewodniczanski Institute of Nuclear Physics, Polish Academy of Sciences, Cracow, Poland
⁴²Institut für Kernphysik, Westfälische Wilhelms-Universität Münster, Münster, Germany
⁴³Joint Institute for Nuclear Research (JINR), Dubna, Russia
⁴⁴Niels Bohr Institute, University of Copenhagen, Copenhagen, Denmark
⁴⁵Institut Pluridisciplinaire Hubert Curien (IPHC), Université de Strasbourg, CNRS-IN2P3, Strasbourg, France
⁴⁶Wayne State University, Detroit, Michigan, United States
⁴⁷Petersburg Nuclear Physics Institute, Gatchina, Russia
⁴⁸Physics Department, University of Jammu, Jammu, India
⁴⁹Laboratori Nazionali di Frascati, INFN, Frascati, Italy
⁵⁰Dipartimento di Fisica dell'Università and Sezione INFN, Padova, Italy
⁵¹Faculty of Nuclear Sciences and Physical Engineering, Czech Technical University in Prague, Prague, Czech Republic
⁵²Nikhef, National Institute for Subatomic Physics, Amsterdam, Netherlands
⁵³Centro de Investigaciones Energéticas Medioambientales y Tecnológicas (CIEMAT), Madrid, Spain
⁵⁴University of Houston, Houston, Texas, United States
⁵⁵Moscow Engineering Physics Institute, Moscow, Russia

- ⁵⁶*Institute for High Energy Physics, Protvino, Russia*
⁵⁷*Faculty of Science, P.J. Šafárik University, Košice, Slovakia*
⁵⁸*Saha Institute of Nuclear Physics, Kolkata, India*
⁵⁹*Institut de Physique Nucléaire d'Orsay (IPNO), Université Paris-Sud, CNRS-IN2P3, Orsay, France*
⁶⁰*Department of Physics, University of Oslo, Oslo, Norway*
⁶¹*Dipartimento di Fisica dell'Università and Sezione INFN, Trieste, Italy*
⁶²*Faculty of Mathematics, Physics and Informatics, Comenius University, Bratislava, Slovakia*
⁶³*Russian Federal Nuclear Center (VNIIEF), Sarov, Russia*
⁶⁴*Physikalisches Institut, Ruprecht-Karls-Universität Heidelberg, Heidelberg, Germany*
⁶⁵*Physics Department, University of Cape Town, iThemba LABS, Cape Town, South Africa*
⁶⁶*Hua-Zhong Normal University, Wuhan, China*
⁶⁷*Sección Física, Departamento de Ciencias, Pontificia Universidad Católica del Perú, Lima, Peru*
⁶⁸*Physics Department, Creighton University, Omaha, Nebraska, United States*
⁶⁹*Université de Lyon, Université Lyon 1, CNRS/IN2P3, IPN-Lyon, Villeurbanne, France*
⁷⁰*Universidade Estadual de Campinas (UNICAMP), Campinas, Brazil*
⁷¹*Nikhef, National Institute for Subatomic Physics and Institute for Subatomic Physics of Utrecht University, Utrecht, Netherlands*
⁷²*Division of Experimental High Energy Physics, University of Lund, Lund, Sweden*
⁷³*University of Tsukuba, Tsukuba, Japan*
⁷⁴*Sezione INFN, Cagliari, Italy*
⁷⁵*Centro de Investigación y de Estudios Avanzados (CINVESTAV), Mexico City and Mérida, Mexico*
⁷⁶*Benemérita Universidad Autónoma de Puebla, Puebla, Mexico*
⁷⁷*Dipartimento di Scienze e Tecnologie Avanzate dell'Università del Piemonte Orientale and Gruppo Collegato INFN, Alessandria, Italy*
⁷⁸*Instituto de Ciencias Nucleares, Universidad Nacional Autónoma de México, Mexico City, Mexico*
⁷⁹*Laboratori Nazionali di Legnaro, INFN, Legnaro, Italy*
⁸⁰*Institute of Space Sciences (ISS), Bucharest, Romania*
⁸¹*Institute of Physics, Bhubaneswar, India*
⁸²*Universidade de São Paulo (USP), São Paulo, Brazil*
⁸³*Dipartimento di Fisica 'E.R. Caianiello' dell'Università and Gruppo Collegato INFN, Salerno, Italy*
⁸⁴*Sezione INFN, Bari, Italy*
⁸⁵*Dipartimento di Fisica dell'Università and Sezione INFN, Cagliari, Italy*
⁸⁶*Soltan Institute for Nuclear Studies, Warsaw, Poland*
⁸⁷*Sezione INFN, Rome, Italy*
⁸⁸*Faculty of Engineering, Bergen University College, Bergen, Norway*
⁸⁹*Institute for Nuclear Research, Academy of Sciences, Moscow, Russia*
⁹⁰*Sezione INFN, Trieste, Italy*
⁹¹*Physics Department, University of Athens, Athens, Greece*
⁹²*Warsaw University of Technology, Warsaw, Poland*
⁹³*Universidad Autónoma de Sinaloa, Culiacán, Mexico*
⁹⁴*Technical University of Split FESB, Split, Croatia*
⁹⁵*Yerevan Physics Institute, Yerevan, Armenia*
⁹⁶*University of Tokyo, Tokyo, Japan*
⁹⁷*Department of Physics, Sejong University, Seoul, South Korea*
⁹⁸*Lawrence Berkeley National Laboratory, Berkeley, California, United States*
⁹⁹*Indian Institute of Technology, Mumbai, India*
¹⁰⁰*Institut für Kernphysik, Technische Universität Darmstadt, Darmstadt, Germany*
¹⁰¹*Yonsei University, Seoul, South Korea*
¹⁰²*Zentrum für Technologietransfer und Telekommunikation (ZTT), Fachhochschule Worms, Worms, Germany*
¹⁰³*California Polytechnic State University, San Luis Obispo, California, United States*
¹⁰⁴*China Institute of Atomic Energy, Beijing, China*
¹⁰⁵*Institute of Physics, Academy of Sciences of the Czech Republic, Prague, Czech Republic*
¹⁰⁶*University of Tennessee, Knoxville, Tennessee, United States*
¹⁰⁷*Dipartimento di Fisica dell'Università "La Sapienza" and Sezione INFN, Rome, Italy*
¹⁰⁸*Hiroshima University, Hiroshima, Japan*
¹⁰⁹*Lawrence Livermore National Laboratory, Livermore, California, United States*
¹¹⁰*Budker Institute for Nuclear Physics, Novosibirsk, Russia*
¹¹¹*Physics Department, University of Rajasthan, Jaipur, India*
¹¹²*Purdue University, West Lafayette, Indiana, United States*
¹¹³*Centre de Calcul de l'IN2P3, Villeurbanne, France*
¹¹⁴*Pusan National University, Pusan, South Korea*

^aDeceased.

^bAlso at Laboratoire de Physique Corpusculaire (LPC), Clermont Université, Université Blaise Pascal, CNRS-IN2P3, Clermont-Ferrand, France.

^cPresent address: Centro Fermi-Centro Studi e Ricerche e Museo Storico della Fisica “Enrico Fermi”, Rome, Italy; Present address: European Organization for Nuclear Research (CERN), Geneva, Switzerland.

^dAlso at European Organization for Nuclear Research (CERN), Geneva, Switzerland.

^ePresent address: Physikalisches Institut, Ruprecht-Karls-Universität Heidelberg, Heidelberg, Germany.

^fPresent address: Sezione INFN, Turin, Italy.

^gPresent address: University of Houston, Houston, TX, USA.

^hAlso at Dipartimento di Fisica Sperimentale dell’Università and Sezione INFN, Turin, Italy.

ⁱAlso at Dipartimento di Fisica dell’Università, Udine, Italy.

^jPresent address: SUBATECH, Ecole des Mines de Nantes, Université de Nantes, CNRS-IN2P3, Nantes, France.

^kPresent address: Centro de Investigación y de Estudios Avanzados (CINVESTAV), Mexico City and Mérida, Mexico; Present address: Benemérita Universidad Autónoma de Puebla, Puebla, Mexico.

^lPresent address: Laboratoire de Physique Subatomique et de Cosmologie (LPSC), Université Joseph Fourier, CNRS-IN2P3, Institut Polytechnique de Grenoble, Grenoble, France.

^mPresent address: Institut Pluridisciplinaire Hubert Curien (IPHC), Université de Strasbourg, CNRS-IN2P3, Strasbourg, France.

ⁿPresent address: Sezione INFN, Padova, Italy.

^oAlso at Division of Experimental High Energy Physics, University of Lund, Lund, Sweden.

^pAlso at University of Technology and Austrian Academy of Sciences, Vienna, Austria.

^qPresent address: Oak Ridge National Laboratory, Oak Ridge, TN, USA.

^rPresent address: European Organization for Nuclear Research (CERN), Geneva, Switzerland.

^sAlso at Wayne State University, Detroit, MI, USA.

^tAlso at Frankfurt Institute for Advanced Studies, Johann Wolfgang Goethe-Universität Frankfurt, Frankfurt, Germany.

^uPresent address: Frankfurt Institute for Advanced Studies, Johann Wolfgang Goethe-Universität Frankfurt, Frankfurt, Germany.

^vPresent address: Research Division and ExtreMe Matter Institute EMMI, GSI Helmholtzzentrum für Schwerionenforschung, Darmstadt, Germany.

^wAlso at Fachhochschule Köln, Köln, Germany.

^xAlso at Institute of Experimental Physics, Slovak Academy of Sciences, Košice, Slovakia.

^yPresent address: Instituto de Ciencias Nucleares, Universidad Nacional Autónoma de México, Mexico City, Mexico.

^zPresent address: Research Division and ExtreMe Matter Institute EMMI, GSI Helmholtzzentrum für Schwerionenforschung, Darmstadt, Germany.

^{aa}Also at Laboratoire de Physique Subatomique et de Cosmologie (LPSC), Université Joseph Fourier, CNRS-IN2P3, Institut Polytechnique de Grenoble, Grenoble, France.

^{bb}Also at “Vinča” Institute of Nuclear Sciences, Belgrade, Serbia.

^{cc}Also at Dipartimento di Fisica Sperimentale dell’Università and Sezione INFN, Turin, Italy.

^{dd}Also at Instituto de Ciencias Nucleares, Universidad Nacional Autónoma de México, Mexico City, Mexico.

^{ee}Also at University of Houston, Houston, TX, USA.

^{ff}Also at Department of Physics, University of Oslo, Oslo, Norway.

^{gg}Present address: Department of Physics, University of Oslo, Oslo, Norway.

^{hh}Also at Eberhard Karls Universität Tübingen, Tübingen, Germany.

ⁱⁱAlso at Dipartimento Interateneo di Fisica ‘M. Merlin’ and Sezione INFN, Bari, Italy.

^{jj}Present address: Nikhef, National Institute for Subatomic Physics and Institute for Subatomic Physics of Utrecht University, Utrecht, Netherlands.

^{kk}Also at Hua-Zhong Normal University, Wuhan, China.

^{ll}Also at Centro Fermi-Centro Studi e Ricerche e Museo Storico della Fisica “Enrico Fermi”, Rome, Italy.